PHYSICAL REVIEW A VOLUME 34, NUMBER 1 JULY 1986

Charge transfer and excitation processes in *p*-He collisions studied using a unified atomic-orbital—molecular-orbital matching method

M. Kimura
Joint Institute for Laboratory Astrophysics, University of Colorado and National Bureau of Standards, Boulder, Colorado 80309

C. D. Lin
Department of Physics, Cardwell Hall, Kansas State University, Manhattan, Kansas 66506

(Received 7 October 1985)

A comprehensive theoretical study of the charge transfer to hydrogen $1s$, $2s$, and $2p$ states and excitation to helium $2\,^1S$ and $2\,^1P$ states in *p*-He collisions in the 1—100 keV energy region is presented. This study is the first demonstration of the application of the recently developed atomic-orbital—molecular-orbital matching procedure to two-electron collision systems. In this method the time-dependent electronic wave function is expanded in terms of traveling atomic orbitals of the two collision centers at large internuclear separation which is matched to the solution in the inner region where it is expanded in terms of molecular orbitals without translation factors. It is shown that the results from the present theoretical method are in good agreement with experimental measurements of (1) total charge-transfer cross sections to $1s$, $2s$, and $2p$ states, (2) charge-transfer probabilities at small impact parameters or large scattering angles, and (3) excitation cross sections to $2\,^1S$ and $2\,^1P$ states above 20 keV.

I. INTRODUCTION

Excitation and charge-transfer processes in proton-helium collisions have been the subject of many experimental studies over the years. A relatively complete set of data for total charge-transfer cross sections to the hydrogenic $1s$, $2s$, and $2p$ states were accumulated in the late 1960s and early 1970s.[1–11] There also have been many differential cross-section measurements.[3–5] For example, the electron capture probability P_0 for close encounters between proton and helium has been measured in the scattering angle from 0.5 to 4 degrees. This corresponds to impact parameters from 0.015 to 0.5 Å in the 1.6—180 keV incident proton energy region. These early measurements sparked the theoretical study by Lichten[12] in which a simple two-state model was proposed to interpret the observed oscillatory charge-transfer probabilities versus reciprocal collision velocity. Later similar measurements by Jaecks and co-workers[10–11] for capture to $2s$ and $2p$ states showed similar oscillatory dependence, though here the simple two-state model of Lichten[12] is no longer applicable.

Since these early measurements, there have been several theoretical calculations[13–16] using basis-function expansion methods as well as perturbation treatments aimed at predicting these experimental results. However, the agreement of these theoretical results with experimental data has been very unsatisfactory except for the most recent elaborate molecular-orbital calculation.[16] In this paper, we will demonstrate that these early data can be understood as well as predicted in *ab initio* calculations using the recently propose unified atomic-orbital—molecular-orbital (AO-MO) matching method. This study serves as the first application of this method to two-electron systems.

Almost all of the theoretical models for describing ion-atom collisions in the keV to MeV region use the semiclassical impact-parameter formulation and expand the time-dependent electronic wave functions in terms of stationary molecular orbitals (MO) or of traveling atomic orbitals (AO) of the collision partners. In the conventional MO expansion, i.e., the so-called perturbed-stationary-state (PSS) approximation, the method does not incorporate the translational motion of the electrons in the asymptotic regions and thus the results are not Galilean invariant. This fundamental deficiency in the PSS method can usually be remedied by incorporating some forms of the molecular electron translation factors (MO-ETF's) into the scattering wave function.[17] No such difficulties exist if the wave functions are expanded in terms of traveling atomic orbitals. However, the AO expansion does not employ the conceptual PSS model. Thus, a unified AO-MO matching method for treating ion-atom collisions was proposed recently by us[18,19] and by Winter and Lane.[20] In this model the time-dependent electronic wave functions are expanded using the atomic orbitals of the two moving centers at large internuclear separations. In the interaction region the wave functions are expanded in terms of molecular orbitals. The solutions in the two regions are matched twice, once in the incoming part and again in the outgoing part of the collision. This method has now been applied to one-electron collision systems such as p-He$^+$,[18] p-H,[19] C^{6+} + H,[19] and He^{2+}-H.[20] The results of these studies were shown to be in good agreement with experiments and with large-scale close-coupling calculations based either on the AO expansion or on the

MO expansion. In this paper, we have generalized the method to two-electron collision systems. We chose *p*-He collisions since there are more detailed experimental data available for comparison.

In Sec. II we discuss the calculation of molecular orbitals and atomic orbitals used in the present study. Since there are no exact molecular or atomic wave functions available for two-electron systems, a description of the approximate wave functions used is necessary. We then describe briefly the matching procedure. In Sec. III, we present the results for the total charge transfer cross sections to 1*s*, 2*s*, and 2*p* states as well as the differential capture probabilities and compare them with experimental data. We also present excitation results and compare them with the limited experimental data. The conclusion is given in Sec. IV.

II. COMPUTATIONAL METHOD

A. Basis set

Accurate eigenfunctions and eigenvalues of the nonrelativistic electronic Hamiltonian of the molecular system is essential to the accurate treatment in the MO-expansion calculation of the scattering wave function. In some cases like the present proton-helium system, the most important collision dynamics take place at small internuclear separation *R*. This requires that we obtain accurate wave functions at small *R* in order to describe the collision properly. To construct molecular wave functions, the linear combination of the Slater determinant approach has been employed with extended Slater-type orbital (STO) basis. Full configuration-interaction (CI) calculations including single and double excitation configurations were performed. Values of the orbital exponents used for the STO's are listed in Table I. Adiabatic potential curves and a diabatic correlation diagram are displayed in Figs. 1(a) and 1(b), respectively. Important couplings are also indicated in Fig. 1(b). The accuracies of all the calculated energies are within 0.05 eV of the spectroscopic values for all states (six Σ and two Π states) considered.

The basis functions used in the outer region ($R > R_c$) are traveling atomic orbitals of the two collision centers where the electron translation factor associated with each atomic orbital is the Bates-McCarroll-type plane-wave phase factor. The stationary one-electron atomic orbitals are known exactly, but the two-electron wave functions of the helium atom have to be calculated approximately. They are expanded in terms of extended STO's. Values of the orbital exponents for the STO's are tabulated in Table II. The energy levels for the $1\,^1S$, $2\,^1S$, and $2\,^1P$ states of He thus calculated are within 1% of the spectroscopic data. These helium atomic orbitals, together with the atomic 1*s*, 2*s*, 2*p*, and 3*p* orbitals of hydrogen atoms are used in the two-center AO expansion in the outer region. The H(3*p*) orbital was added in the basis to partially account for the flux loss to higher Rydberg states and to the continuum. For a given collision, there is a small amount of diffuse charge cloud which would end up in the Rydberg states and in the continuum states at the end of the collision. In close-coupling calculations, since only bound states are used in the basis expansion, these small diffuse

TABLE I. Orbital exponents of the STO basis functions.

	He		H
1*s*	4.346	1*s*	5.000
	2.780		2.000
	1.453		1.000
			0.50
2*s*	5.30	2*s*	5.00
	3.40		1.00
	1.52		0.50
	1.00		
2*p*	4.30	2*p*	5.00
	2.40		1.00
	1.50		0.50

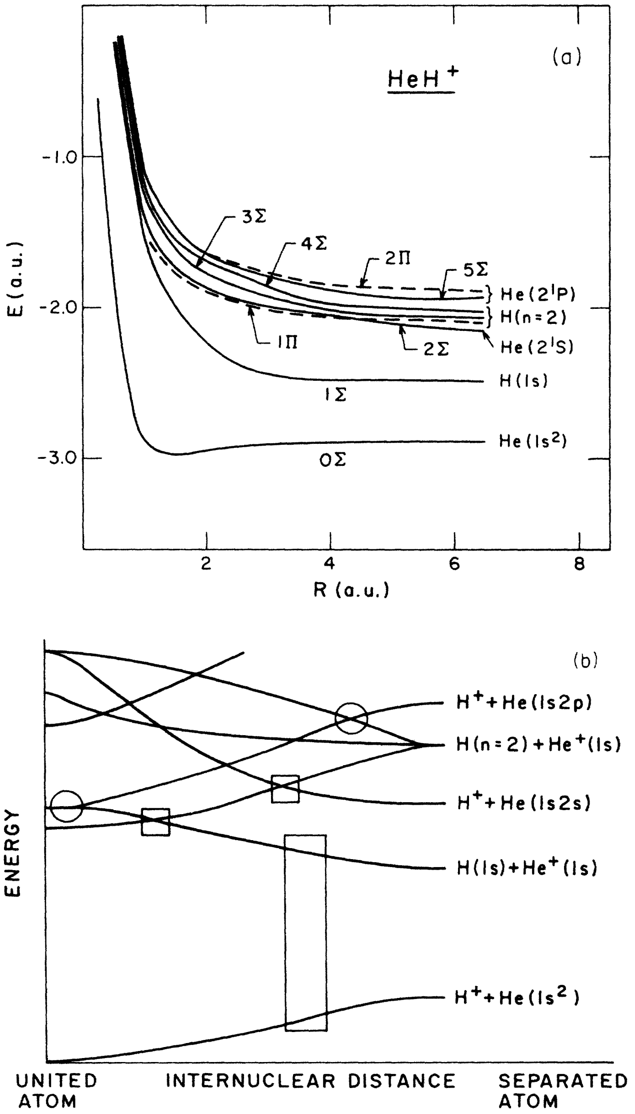

FIG. 1. (a) Adiabatic potentials for the (H-He)$^+$ system. (b) Diabatic correlation diagram for the (H-He)$^+$ system. Important radial as well as rotational couplings are indicated by boxes and circles, respectively.

TABLE II. Orbital exponents for the He atomic orbitals.

1s	2s	2p
7.0	6.0	5.0
2.0	4.0	3.0
1.0	1.0	1.0

electron clouds are reflected back to the bound states resulting in an overestimate of the probabilities to these states. One procedure[21] to amend this situation is to introduce some diffuse states in the expansion such that the diffuse charge cloud would reflect back to the additional diffuse orbitals included. The H(3p) orbital is the most diffuse one included in our basis expansion. We did not extend to a larger basis set since such effect is not very large in the present energy range studied.

B. Coupled equations

Within the semiclassical formulation, the scattering wave function of a collision system is expanded in terms of a set of basis functions, $\{U_i(\mathbf{r},t)\}$, as

$$\psi(\mathbf{r},t)=\sum_i a_i(t)U_i(\mathbf{r},t)\ , \tag{1}$$

where $\mathbf{r}$ denotes collectively the position vectors of the electrons. Substituting Eq. (1) into the time-dependent Schrödinger equation we obtain a set of linear coupled equations,

$$i\underline{S}\dot{\underline{A}}=\underline{M}\underline{A}\ , \tag{2}$$

where the column matrix $\underline{A}$ represents the time-dependent expansion coefficients, $\underline{S}$ is the overlap matrix with elements $S_{ij}=\langle U_i\mid U_j\rangle$, and $\underline{M}$ is the coupling matrix with elements $M_{ij}=\langle U_i\mid H_{\text{el}}-i\partial/\partial t\mid U_j\rangle$, where H_{el} is the electronic Hamiltonian of the system.

In the AO-MO matching approach, the internuclear separation (or the time axis) is divided into two regions: The outer region where the charge cloud from each atomic center overlaps only slightly and the inner region where the charge cloud is shared by the two centers. In the outer region, the electron cloud around each atomic center can be expected to travel mostly with that center. Thus in the outer region the conventional two-center AO-expansion model is a more appropriate approximation for the description of a collision system and the scattering wave function is expanded using the AO representation,

$$\psi^{\text{out}}(\mathbf{r},t)=\sum_i a_i(t)\tilde{\phi}_i^{\text{AO}}(\mathbf{r})+\sum_j b_j(t)\tilde{\phi}_j^{\text{AO}}(\mathbf{r})\ , \tag{3}$$

where $\tilde{\phi}_i^{\text{AO}}(\mathbf{r})$ is a traveling orbital in a form of a Slater determinant and i and j refer to excitation and charge-transfer channels, respectively. Note that the potential interaction due to the two collision centers is the source of the coupling matrix in the AO representation. The set of coupled equations (2) derived from using the scattering wave function (3) are integrated from $-\infty$ to $-t_0$.

In the inner region, the electron cloud is shared by the two collision centers and there is no *a priori* information about how the electrons are traveling with each center. This region in general should be treated variationally. For slow collisions, we expect that the basic collision dynamics can be described using the molecular-orbital model. In this inner region, the electron cloud is more compact and the kinetic energy of the electron is large compared to the kinetic energy associated with the translational motion. This is true for slow collisions where the incident projectile speed is smaller than the typical orbital speed of the electron. Thus we expand the electronic wave functions in the inner region using molecular orbitals without introducing any electronic translation factors. The scattering wave function (1) in this region is expanded in the MO representation similar to the method of the PSS approximation as

$$\psi^{\text{In}}(\mathbf{r},t)=\sum_k c_k(t)\phi_k^{\text{MO}}(\mathbf{r};\mathbf{R})\ . \tag{4}$$

A set of coupled equations obtained by the scattering wave function (4) should be integrated from $-t_0$ to $+t_0$. The nonadiabatic coupling is the source of transition from one molecular state to another in this representation.

In the exit part the scattering wave function is again expanded in terms of two-center traveling AO's in the same manner as in the entrance and the resulting coupled equations (2) should be integrated from $+t_0$ to $+\infty$ to extract transition amplitudes for the state of interest. The probability for excitation to state m is $|a_m(+\infty)|^2$ and for capture to state n is $|b_n(+\infty)|^2$.

At the two matching points, it is assumed that the scattering wave function can be represented by either expansion. Thus the known scattering wave function calculated in one representation is used to calculate the unknown expansion coefficients in another representation. For example, at $-t_0$, the scattering wave function calculated from the AO expansion $\psi^{\text{out}}(\mathbf{r},t)$ is projected onto each MO to yield

$$c_k(-t_0)=\langle\phi_k^{\text{MO}}(\mathbf{r},R_0)\mid\psi^{\text{out}}(\mathbf{r},t)\rangle\ , \tag{5}$$

where $R_0=R(-t_0)$. These coefficients serve as the initial condition for the integration of the coupled equations in the MO representation. In the outgoing part of the collision at $+t_0$, the calculated scattering wave function in the inner region, $\psi^{\text{in}}(\mathbf{r},t)$, from the MO expansion, is rewritten by expanding in terms of atomic orbitals of the two centers. The coefficients in the AO expansion at $+t_0$ are obtained by solving the following algebraic equations:

$$a_i(+t_0)=\langle\tilde{\phi}_i^{\text{AO}}\mid\psi^{\text{in}}(\mathbf{r},t_0)\rangle-\sum_j b_j\langle\tilde{\phi}_i^{\text{AO}}\mid\tilde{\phi}_j^{\text{AO}}\rangle\ , \tag{6}$$

$$b_j(+t_0)=\langle\tilde{\phi}_j^{\text{AO}}\mid\psi^{\text{in}}(\mathbf{r},t_0)\rangle-\sum_i a_i\langle\tilde{\phi}_j^{\text{AO}}\mid\tilde{\phi}_i^{\text{AO}}\rangle\ . \tag{7}$$

The solutions of Eqs. (6) and (7) provide the initial conditions needed to integrate the coupled equations in the AO representation from $+t_0$ to $+\infty$ to extract scattering amplitudes.

The probability $P_i(E,b)$ for electron capture to a particular jth state is given by

$$P_j(E,b)=|b_j(+\infty)|^2 \tag{8}$$

and electron capture cross section σ_j is defined as

$$\sigma_j(E)=2\pi\int_0^\infty db\, bP_j(E,b)\ . \tag{9}$$

C. Numerical accuracies

The coupled equations (2) were solved numerically by the method of Bulirsh and Stoer[22] with a relative truncation error automatically maintained between 10^{-5} and 10^{-6} in both MO and AO regions. The cross section was computed by trapezoidal integration to at least 1% accuracy. Apart from these minor inaccuracies in the numerical procedure, the present frame-transformation approach contains two inherent problems, namely the sensitivity of the calculated probabilities with respect to the matching radius R_0 and the loss of unitarity at the matchings. The matching radius R_0 was chosen at the smallest R where the molecular orbitals can still be well expressed in the linear combination of atomic orbitals (LCAO) manner. This matching R_0 in the present case corresponds roughly from 1.5 to 2.0 a.u.

Within this range the calculated probabilities are relatively stable for energies below 20 keV. For the dominant H(1*s*) capture cross section, the difference due to the change of R_0 is less than 2%. For the small capture channel, i.e., to H(2*s*), the difference is about 11%. The difference for the excitation to He($2\,^1P$) is larger, being about 30% at the highest energy studied. This stronger dependence may be attributed to the fact that the basis size used in this calculation is relatively small (eight MO's in the inner region). Since very few diffuse orbitals are included in the calculation, the energetically highest state, He($2\,^1P$), which is also quite diffuse, is the one affected the most by the matching radius chosen. It is expected that this sensitivity will be reduced if the basis size is enlarged.

Another inherent numerical feature is the loss of unitarity of the total probability at the matching point. This is due to the fact that the two sets of basis functions used at the matching point are not complete. The loss of unitarity in the present case is generally less than 18% at the highest-energy point studied. This value is relatively high compared to our previous studies on $\mathrm{H}^+ + \mathrm{H}$ and $\mathrm{C}^{6+} + \mathrm{H}$ systems. This may be mostly due to the small basis size used in the present calculation. At the higher energies, part of the loss of unitarity can be attributed to ionization events. The loss of unitarity in the calculation indeed increases with increasing collision energies. On the other hand, the limited number of molecular orbitals used in the inner region also becomes less adequate as the collision energy increases.

D. Molecular ETF's

In the MO representation, the electron is regarded as not belonging to either nucleus, but shared by both at small internuclear separations. Accordingly, the ETF should contain some information about how an electron is attached. This makes the determination of the molecular ETF's more complicated, in contrast to the atomic ETF's which are defined uniquely. In the present collision system, the processes considered are very sensitive to the dynamic coupling at small R ($R \lesssim 1$ a.u.). We speculate that the charge-transfer and excitation results are very sensitive to the form of the molecular ETF (MO-ETF) chosen in the calculation. Indeed, as we will discuss later, probabilities of H($n=2$) charge transfer and He($2\,^1P$) excitation are, in particular, sensitive to the form of the MO-ETF used since these processes are preceded by a strong radial coupling between 0Σ and 1Σ at $R\sim 2.0$ a.u.

In the present "full" MO calculation, we have adopted the MO-ETF form

$$F_i^{\mathrm{MO}}(\mathbf{r},R)=\exp\left[i\sum_k\left[\tfrac{1}{2}f_i(\mathbf{r}_k,R)\mathbf{V}\cdot\mathbf{r}_k-\tfrac{1}{8}\int^t v^2\,dt'\right]\right]\ , \tag{10}$$

$$f_i(\mathbf{r}_k,R)=\tanh[R\beta_i(R)r_k]\ , \tag{11}$$

where $f_i(\mathbf{r}_k,R)$ is the so-called state-dependent switching function which represents the two-center character of the MO-ETF.[17] The parameter $\beta_i(R)$ in Eq. (11) was chosen to minimize the nonadiabatic couplings arising in the MO calculation. Its values depend on the state and on R, ranging from 0.01 to 0.89.

If the atomic ETF's were used in the MO expansion, as was done in Ref. 16, our calculations showed that although the total integrated cross sections do not depend on the forms of the molecular ETF's, the impact-parameter dependences of the probabilities do differ by as much as 25% in certain cases.

III. RESULTS AND DISCUSSION

All calculations presented in this section have been made by a semiclassical method with a Coulomb trajectory with charges one and two, respectively, for protons and for helium.

A. Total charge-transfer cross sections

In Fig. 2, we present the charge-transfer cross sections for the H(1*s*) state obtained from the present method and from other theoretical calculations. Also shown are the experimental total capture cross sections which include small contributions from excited states. The experimental data are from the early measurements of Allison,[1] Stedeford and Hasted,[2] and Williams *et al.*[8] Among the theoretical models we only show the results of the four-state AO calculation of Sin Fai Lam[14] and the recent MO calculation of Kimura.[16] There are other calculations which used smaller basis sets.[13] The results of these less elaborate calculations are not shown.

The agreement of the MO calculation with the present one is quite good over the whole energy range. In the MO calculation of Kimura,[16] the electron translational factor is kept to first order in $\mathbf{v}$. It appears that this approximation to the ETF has no significant effect (within 10%) on the calculated capture cross sections (see also Fig. 3). The results of the present calculation and those of the MO expansion agree quite well with experimental data for incident energies above 4 keV, although the theoretical re-

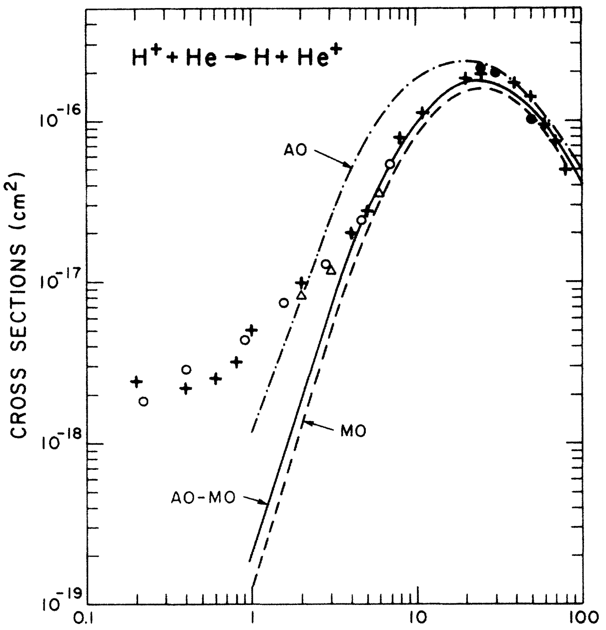

FIG. 2. Charge-transfer cross sections for the H(1s) state. Theory: solid line, present; dashed line, Ref. 16; dash-dotted line, Ref. 14. Experiment: ○, Ref. 1; +, Ref. 2; △, Ref. 8.

sults tend to be slightly below the experimental data. For energies below 4 keV, the discrepancy between theory and experiment is quite large. It appears that the problem lies in the experimental difficulty. From the collision theory viewpoint, at low energies the collision is basically dominated by the radial coupling between the two lowest channels. The transition probability, as predicted by the simple Landau-Zener model or the oscillatory damping model of Lichten,[12] decreases exponentially such that we would expect that the cross section at low energies decreases exponentially. The low-energy experimental data shown in Fig. 2 contradict this general behavior.

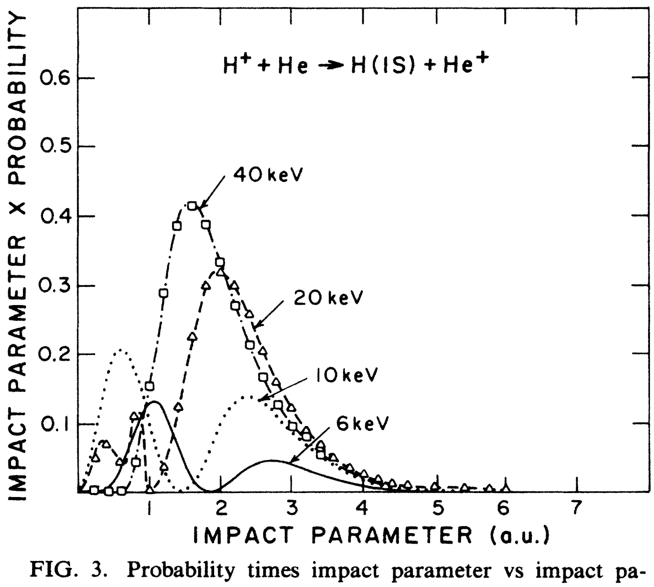

FIG. 3. Probability times impact parameter vs impact parameter for 1s charge transfer with different collision energies.

The four-state AO expansion of Sin Fai Lam[14] as well as the earlier two-state AO expansion of Green *et al.*[13] do not reproduce experimental results and disagree significantly with the present calculation as well as with the MO calculation of Kimura.[16] The AO expansion is not expected to be valid for collisions occurring at small impact parameters, as has been documented by many theoretical studies for one-electron systems.[23] In Fig. 3, the weighted probabilities versus impact parameters are shown at four different energies. We note that for $E < 10$ keV, about half of the total capture cross section comes from impact parameters less then 2 a.u. The AO expansion does not describe collisions at small impact parameters[23] and thus the calculated total cross section is inaccurate. At higher energies, i.e., near the peak, the AO results are less inaccurate because of the large contribution from larger impact parameters.

B. Charge-transfer probability at large scattering angles

In their pioneering work, Helbig and Everhart[4] measured the charge-transfer probability in H^+-He collisions at large scattering angles. When the capture probability is plotted versus the reciprocal velocity of the incident ion, a damped oscillatory structure was observed. This oscillatory structure was described by Lichten[12] in terms of a semiempirical two-state PSS model. His result for close collisions is given by the expression

$$P = e^{-v/v_0}[\sin^2(\langle Ea \rangle /2v - \beta)] , \qquad (12)$$

where the parameters are $\langle Ea \rangle = 5.71$, $v_0 = 0.85$, and $\beta = 45^\circ$ for $H^+ + He$ collisions by fitting the experimental data to Eq. (12). Lichten's work explained qualitatively the origin of the oscillatory structure as being similar to the oscillations observed in resonant capture but the structure has not been explained using *ab initio* calculations. There are at least two reasons. Firstly, accurate molecular potential curves and coupling terms are relatively difficult to calculate. Secondly, the familiar problem associated with the electron-translation factors in the PSS approximation makes the standard PSS calculations completely invalid. Thus, we are faced with the dilemma that a simple qualitative explanation of the oscillatory structure is possible, but no quantitative calculations based on first principles is possible.

In Fig. 4 we show the total capture probability versus the reciprocal velocity for collisions at $\rho = 0.14$ a.u. or $\theta T = 20$ keV deg. The experimental data of Helbig and Everhart[4] are compared with the results of the present calculation with a straight-line trajectory, with a Coulomb trajectory, and with the present MO calculation. We note that the oscillatory structure is well reproduced by the three calculations. Notice also that in each model the molecular orbitals are used in the inner region. The MO model uses linearized (in v) MO-ETF's throughout the whole region, while the present method is identical to the PSS model in the inner region and the outer region is represented by traveling atomic orbitals. None of the calculations presented here have the origin-dependence problem of the PSS model. Furthermore, the trajectory effect is obvious in the lower energy side.

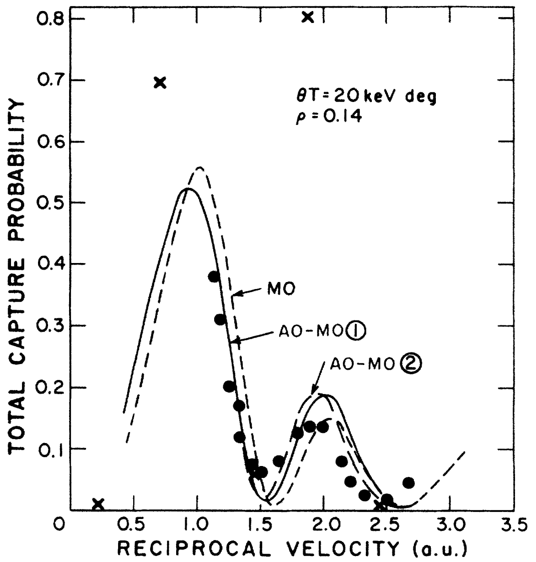

FIG. 4. Total capture probability vs reciprocal velocity for collision at $\rho=0.14$ a.u. or $\theta T=20$ keV deg. Theory: AO-MO curve 1, present linear trajectory; AO-MO curve 2, present curved trajectory; MO, present; the position and magnitude of the maxima and minima of the oscillatory structure predicted by Ref. 14, ×. Experiment: ●, Ref. 4.

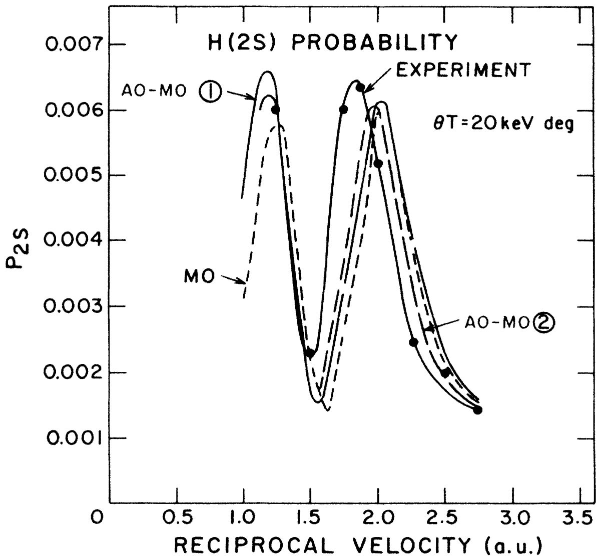

FIG. 5. Capture probability to H(2S) state vs reciprocal velocity. Theory: AO-MO curve 1, present linear trajectory; AO-MO curve 2, present curved trajectory; MO, present. Experiment: solid line, Ref. 10.

We have not compared the experimental results with the AO-based calculations of Sin Fai Lam.[14] As indicated earlier, the AO expansion is not expected to be valid for describing collisions at small impact parameters. In Fig. 4 we indicated the position and magnitude of the maxima and minima of the oscillatory structure predicted according to the AO model. It is clear that the latter model does not provide an adequate description of the data. (A detailed comparison of the data with earlier calculations can be found in Fig. 6 of Ref. 10.)

This comparison clearly demonstrated that the basic MO interpretation of the dominant capture process is correct, despite the fact that a satisfactory detailed calculation based on first principles is more difficult. The question still to be answered is whether the weaker capture channels can also be confirmed by these calculations. For the capture to excited 2s and 2p states the processes cannot be described by a two-state model.

C. Charge-transfer probability to H(2s) at large scattering angles

The excitation mechanism for charge transfer to 2s is definitely not a two-channel process. One would expect that at low collision energies the electron is first promoted to 1Σ channel via radial coupling, i.e., the same coupling which populates the H(1s) channel, followed by the radial coupling with 2Σ which is further coupled with the 3Σ channel. Since asymptotically the H(2s) and H(2p) states are degenerate, there is a significant amount of Stark mixing in the outgoing leg of the collision. This clearly demonstrates that the population of H(2s) in the collision process is quite complicated. The three-stage mechanism discussed above, although expected to be the dominant excitation mechanism at low energies, is not necessarily the only important one at higher energies. It is not clear, for example, how important the two-step (or the one-step) mechanism is. In one of the possible two-step processes, for example, the electron can be promoted from 0Σ to 2Σ and then couple to 3Σ. It is likely that the relative importance depends on the collision speed as well as on impact parameters.

The capture probability to H(2s) at large scattering angles has been investigated by Crandall and Jaecks,[10] as well as by others. The capture probability to H(2s) obtained by Crandall and Jaecks[10] versus the reciprocal velocity is displayed in Fig. 5. The oscillatory structure is quite obvious, even though the capture probability is only a fraction of a percent. The presence of the well-behaved oscillatory structure indicates that the possible complicated multistep couplings do not wash away the oscillation. This can be understood from the fact that the oscillation is a feature of the charge cloud of the collision system (see also Fig. 10). The oscillatory structure of each state reflects the oscillation of the charge cloud between the two nuclei. It is possible that this oscillation can be observed for higher states too. Note that the trajectory effect which is apparent at lower energies disappears as the energy increases.

D. Total H(2s) capture cross sections

In Fig. 6 we show the total H(2s) capture cross sections from 2–100 keV. The results from the various experimental data are in good agreement with each other. The present calculation and the MO result of Kimura[16] are in good agreement with experimental data. Although measured cross sections[10] show some structures around 6–10 keV, no such structures are evident in the calculated results.

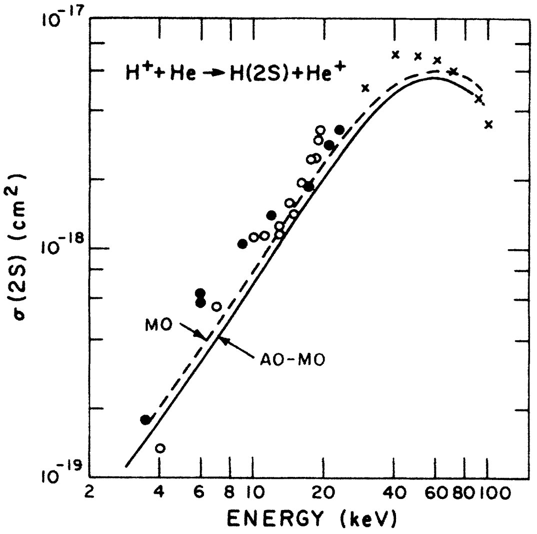

FIG. 6. Total H(2S) capture cross section. Theory: solid line, AO-MO; broken line, MO; both present. Experiment: ○, Ref. 10; ●, Ref. 7; ×, Ref. 9.

E. Capture probability to H(2p) at large scattering angles

The probability for electron capture to H(2p) at large scattering angles has been measured by McKnight and Jaecks.[11] Their results for $\rho=0.138$ a.u. or $\theta T=20$ keV deg are shown in Fig. 7, together with the predictions from the present MO calculation and of the present AO-MO matching study. The general agreement is quite good except that the maximum in the theoretical results near $1/v=2.0$ is much sharper than the experimental data have indicated. It is surprising that the agreement is not better here since good agreement has been achieved for the corresponding probability for H(2s); note in particular that the probabilities for H(2p) are about ten times larger than the result for H(2s) at this energy. Since the theoretical results for H(2s) and for H(2p) are obtained in a single calculation, it is suggested that further experimental data are needed to understand the discrepancy in Fig. 7.

We have not shown the results from the work of Sin Fai Lam in Fig. 7. His AO results are about a factor of 10 too high in comparison with experimental data, although the phase of the oscillation is about the same.

F. Total H(2p) capture cross sections

Total capture cross sections to H(2p) are shown in Fig. 8 from 2—100 keV. The experimental data of Jaecks *et al.*[7] in the 6—25 keV region are well reproduced by the present calculation. Their low-energy results for $E<4$ keV appear to be too high, see Fig. 2. The results of de Heer *et al.*[6] also appear to be too high in the 10—30 keV range. There are noticeable discrepancies between the two calculations and experimental data at higher energies. We tend to believe that the problems are in the calculations. For collision energies between 50 and 100 keV the ionization cross section is about 8×10^{-17} cm^2. This is almost 2 orders of magnitude larger than H(2p) capture cross sections. In the theoretical treatment for small capture channels, the effect of the coupling with ionization channels should be included, particularly in this energy region. Previous experience in the one-electron collision systems indicates that the neglect of ionization channels tends to overestimate cross sections for bound states as the flux to the ionization channels is reflected back into bound states. We can see that the effect of ionization channels on H(2s) is less severe in the noted energy region. This is partly because H(2s) cross sections are relatively larger and are less affected by the coupling with the ionization channels.

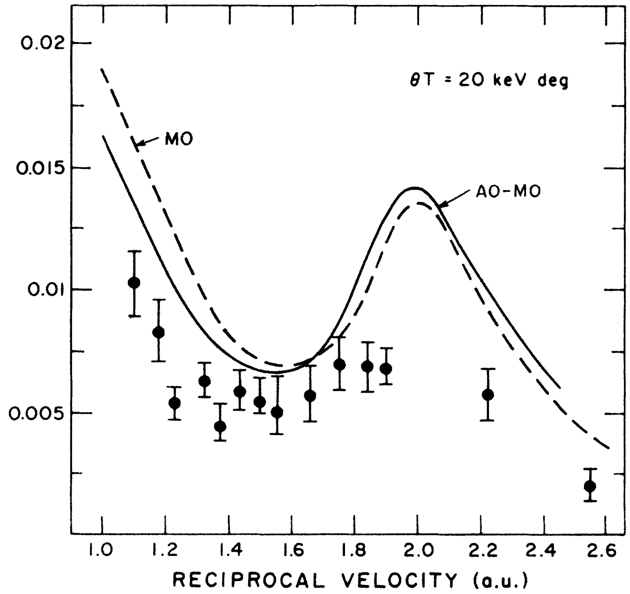

FIG. 7. Capture probability to H(2p) vs reciprocal velocity. Theory: solid line, AO-MO; dashed line, MO; both present. Experiment: ●, Ref. 11.

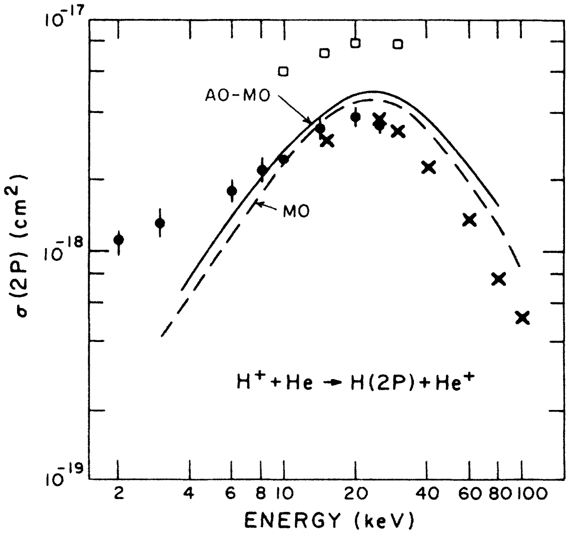

FIG. 8. Total H(2p) capture cross section. Theory: solid line, AO-MO; dashed line, MO; both present. Experiment: ●, Ref. 7; □, Ref. 6; ×, Ref. 9.

G. Total excitation to He($2\,^1S$) and He($2\,^1P$) cross sections

In Figs. 9 and 10 we show the excitation cross sections to the He($2\,^1S$) and He($2\,^1P$) states, respectively. The theoretical results shown are the MO work of Kimura,[16] the one-centered AO calculation of Flannery,[24] and the present AO-MO matching calculation. There are few experimental data for proton energies below 25 keV. The experimental data of Kvale *et al.*[25] above 25 keV have large error bars. At the energies where comparison with experimental data is possible, all the theoretical results are comparable and are in reasonable accord with experimental data. For the lower energies, the AO results of Flannery[24] in general are higher, whereas the MO results of Kimura[16] and the present results are in good accord with each other.

At higher energies, say above 50 keV, one would expect that excitations to $2\,^1S$ and $2\,^1P$ states of He come mostly from collisions at larger impact parameters. In this case, the charge-transfer channels do not couple significantly with the excitation channels and the one-centered AO expansion model can be expected to work reasonably. This explains the general agreement between the results of Flannery[24] and the other two calculations at higher energies. At lower collision energies, the one-centered AO expansion is not expected to describe the excitation processes correctly. Referring to the correlation diagram, excitations to $2\,^1S$ or to $2\,^1P$ have to proceed first through the radial coupling between 0Σ and 1Σ at $R = 2.0$ a.u., then via additional radial and rotational couplings to the final excitation states. This stepwise flux promotion mechanism is not described in the one-centered AO expansion[23] of the scattering wave function.

Excitation to the $2\,^1P$ state at low energies can provide a critical test of the present theoretical model since coupling with intermediate channels is expected to be important at low energies. Our results here, as well as the results from the MO work of Kimura,[16] should be considered as preliminary only because of the small MO basis functions used. The difficulty of obtaining very accurate potential curves for the higher channels prevents us from including additional channels in the calculation.

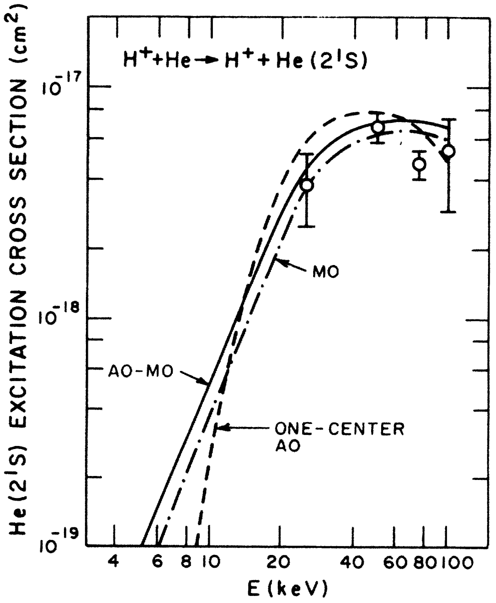

FIG. 9. Total He($2\,^1S$) excitation cross section. Theory: solid line, present AO-MO; dash-dotted line, present MO; dashed line, Ref. 24. Experiment: ○, Ref. 25.

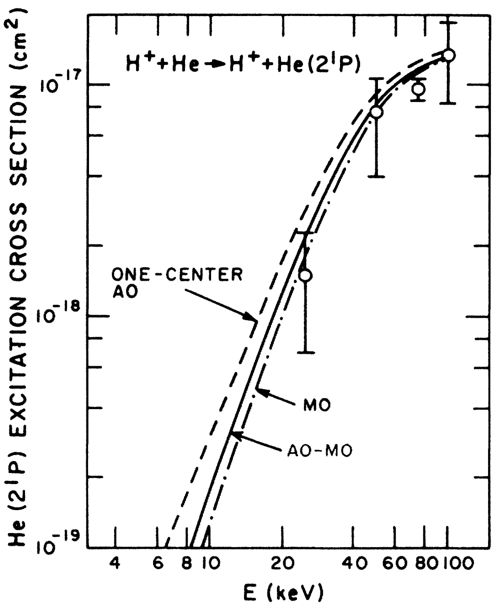

FIG. 10. Total He($2\,^1P$) excitation cross section same as in Fig. 9.

H. Phase mismatch of excitation and charge-transfer probabilities

In low-energy ion-atom collisions, one can expect that the charge cloud separates into two parts, one centered around the target and the other around the projectile, before the electron settles into individual final states. This is due to the long-range behavior of the Coulomb interaction between the two separating aggregates which is still quite strong even after the overlap (or the exchange in-

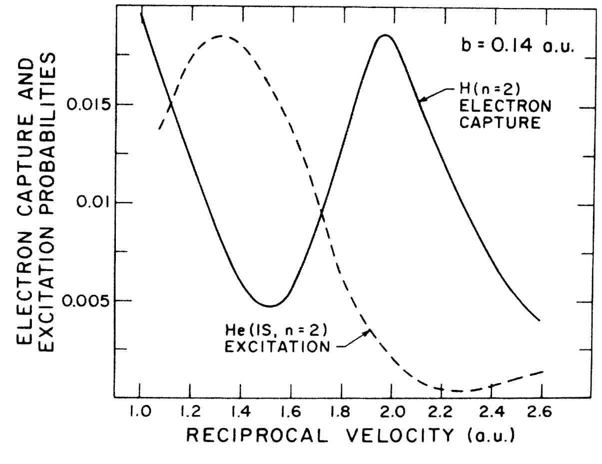

FIG. 11. Electron capture and excitation probabilities vs reciprocal velocity. Note the excitation probability is multiplied by a factor of 2.6.

tegral) between the two centers vanishes. If this simple picture is correct, then we would expect some phase relation between the probability for capture and for excitation, i.e., we would expect that when one is at the maximum the other is at the minimum, and vice versa. To illustrate this behavior, we show in Fig. 11 the total probability of capture to $2s$ and $2p$ of hydrogen and the total excitation probability to $2\,^1S$ and $2\,^1P$ of helium at impact parameter $b=0.14$ a.u. plotted against $1/v$. We notice that the oscillation of the two probabilities is indeed roughly out of phase. No such experimental data have been obtained so far.

IV. CONCLUSIONS

In this article we demonstrated that the AO-MO matching method proposed recently can be easily applied to two-electron collision systems. We have applied the method to study excitation and charge transfer to $2s$ and $2p$ states in proton-helium collisions and have shown that the method is capable of predicting experimental results, not only on total cross sections but also on capture probabilities at small impact parameters. The *ab initio* calculations presented here complement the semiempirical analysis of Lichten[12] where the traditional PSS model was employed. We have demonstrated that the method provides the bridge between the qualitative description of the PSS model and the *ab initio* calculations based on the molecular-orbital models.

The results from the present work appear to indicate that the MO calculations with a linearized approximation on molecular electron-translation factors are not critical to the final answers provided that an optimum MO-ETF is found. Test calculations have shown that, however, the answers are relatively sensitive to the form of the MO-ETF's used. Since most of the differences in the MO-ETF's are in the region where the internuclear separation is small, this relative sensitivity is probably due to the fact that transitions investigated here are dominated by the dynamical coupling at small internuclear separations. The advantage of the present matching procedure is that the optimum form of the MO-ETF's need not be pursued. On the other hand, it is desirable to enlarge the MO basis set used in this type of calculation to test the accuracy of the matching procedure. This requires a large amount of computer time which is prohibitive for us at present.

ACKNOWLEDGMENT

This work was supported in part by the U.S. Department of Energy, Office of Basic Energy Sciences, Division of Chemical Sciences.

---

[1] S. K. Allison, Rev. Mod. Phys. **30**, 1137 (1958).

[2] J. B. H. Stedeford and J. B. Hasted, Proc. R. Soc. London, Ser. A **227**, 466 (1955).

[3] G. J. Lockwood and E. Everhart, Phys. Rev. **125**, 567 (1962).

[4] H. F. Helbig and E. Everhart, Phys. Rev. **140**, A715 (1965); **136**, A674 (1964).

[5] F. P. Ziemba, G. J. Lockwood, G. H. Morgan, and E. Everhart, Phys. Rev. **118**, 1552 (1960).

[6] F. J. de Heer, J. van Eck, and J. Kistemaker, in *Proceedings of the Sixth International Conference on Ionization Phenomena in Gases* (Serma, Paris, 1963), Vol. 1, p. 73.

[7] D. Jaecks, B. van Zyl, and R. Geballe, Phys. Rev. **137**, A340 (1965).

[8] J. F. Williams and D. N. Dunbar, Phys. Rev. **149**, 62 (1966).

[9] R. H. Hughes, E. D. Stokes, S-S. Choe, and T. J. King, Phys. Rev. A **4**, 1453 (1971).

[10] D. H. Crandall and D. H. Jaecks, Phys. Rev. A **4**, 2271 (1971).

[11] R. H. McKnight and D. H. Jaecks, Phys. Rev. A **4**, 2281 (1971).

[12] W. Lichten, Phys. Rev. **131**, 229 (1963); **139**, A27 (1965).

[13] T. A. Green, H. E. Stanley, and Y. C. Chiang, Helv. Phys. Acta **38**, 109 (1965).

[14] L. T. Sin Fai Lam, Proc. Phys. Soc. London **92**, 67 (1967).

[15] T. G. Winter and C. C. Lin, Phys. Rev. A **10**, 2141 (1974).

[16] M. Kimura, Phys. Rev. A **31**, 2158 (1985).

[17] J. B. Delos, Rev. Mod. Phys. **53**, 287 (1981).

[18] M. Kimura and C. D. Lin, Phys. Rev. A **31**, 590 (1985).

[19] M. Kimura and C. D. Lin, Phys. Rev. A **32**, 1357 (1985).

[20] T. G. Winter and N. F. Lane, Phys. Rev. A **31**, 2698 (1985).

[21] W. Fritsch and C. D. Lin, Phys. Rev. A **27**, 3361 (1983).

[22] R. Bulirsch and J. Stoer, Numer. Math. **8**, 1 (1966).

[23] See, for example, W. Fritsch, and C. D. Lin, J. Phys. B **15**, 1255 (1982).

[24] M. R. Flannery, J. Phys. B **3**, 306 (1970).

[25] T. J. Kvale, D. G. Seely, D. M. Blankenship, E. Redd, T. J. Gay, M. Kimura, E. Rille, J. L. Peacher, and J. T. Park, Phys. Rev. A **32**, 1369 (1985).